Quantitative concentration measurements of atomic sodium in an atmospheric hydrocarbon flame with asynchronous optical sampling

Gregory J. Fiechtner, Galen B. King, and Normand M. Laurendeau

We report the development of a pump–probe instrument that uses a high-repetition-rate (82-MHz) picosecond laser. To maximize laser power and to minimize jitter between the pump- and the probe-pulse trains, we choose the asynchronous optical sampling (ASOPS) configuration. Verification of the method is obtained through concentration measurements of atomic sodium in an atmospheric methane–air flame. For the first time to our knowledge, ASOPS measurements are made on a quantitative basis. This is accomplished by calibration of the sodium concentration with atomic absorption spectroscopy. ASOPS measurements are taken at a rate of 155.7 kHz with only 128 averages, resulting in a corresponding detection limit of 5×10^9 cm^{-3}. The quenching-rate coefficient is obtained in a single measurement with a variation of ASOPS, which we call dual-beam ASOPS. The value of this coefficient is in excellent agreement with literature values for the present flame conditions. Based on our quantitative results for detection of atomic sodium, a detection limit of 2×10^{17} cm^{-3} is predicted for the Q_1 (9) line of $A\ ^2\Sigma^+$ ($v = 0$)–$X^2\Pi$ ($v = 0$) hydroxyl at 2000 K. Although this value is too large for practical flame studies, a number of improvements that should lower the ASOPS detection limit are suggested.

Key words: Combustion, turbulence, sodium, picosecond phenomena, mode-locked lasers, absorption, spectroscopy.

1. Introduction

Turbulent combustion is an important factor in many practical energy-conversion devices. Spatially and temporally resolved concentration measurements of minor species in turbulent flames are necessary for improved design of these devices. Laser-induced fluorescence has been widely used to measure concentrations of minor species in flames, including turbulent flames.[1] Unfortunately, laser-induced fluorescence measurements of fluctuating species concentrations are generally limited to probability distribution functions taken at the low repetition rate (~10 Hz) of *Q*-switched laser pulses. As an exception to this observation, consider the laser-induced fluorescence study of Wrobel and Pratt, who used a cw dye laser to excite atomic sodium in a turbulent diffusion flame.[2] In this case the fluorescence signal was analyzed by the recording of power spectral densities from dc to a few kilohertz. However, these fluorescence signals remain inversely proportional to the quenching-rate coefficient Q, thus introducing uncertainty into the data through fluctuations in the collisional environment.[3] We seek to overcome this difficulty by the use of picosecond pump–probe absorption spectroscopy with high-repetition-rate (82-MHz) lasers. In particular we demonstrate the quantitative use of asynchronous optical sampling (ASOPS).

In a companion paper[4] we develop a picosecond pump–probe absorption model. The model has been used to design a series of experiments with the ASOPS instrument, which are described in the present paper. In addition we present the first quantitative evaluation of the ASOPS method in a combustion environment. In this study atomic sodium is seeded into a laminar, atmospheric-pressure hydrocarbon flame. The absolute sodium number density is calibrated with atomic absorption spectroscopy (AAS). Close agreement between the AAS and the ASOPS data concerning the onset of optically thick conditions is observed. The ASOPS data are taken at a beat frequency of 155.7 kHz with only 128 averages. The resulting collection time is sufficient for turbulent

When this research was performed the authors were with the Flame Diagnostics Laboratory, School of Mechanical Engineering, Purdue University, West Lafayette, Indiana 47907. G. J. Fiechtner is now with the Combustion Research Facility, Sandia National Laboratories, Livermore, California 94551.

Received 27 June 1994; revised manuscript received 2 August 1994.

0003-6935/95/061117-10$06.00/0.

fluctuations of ~1 ms or less. The corresponding detection limit is determined based on a 1:1 signal-to-noise ratio (SNR). Although the present results are limited to detection of atomic sodium, our goal is the detection of minor flame species such as hydroxyl and CH. The 1:1 SNR for sodium is thus used in conjunction with the picosecond pump–probe absorption model[4] to estimate the minimum detectability for the hydroxyl radical.

In previous experiments with the ASOPS technique[3] we found that the excited-state decay for atomic sodium was not a single exponential. As a result multiple measurements were necessary to obtain the electronic quenching-rate coefficient for this multilevel absorber–emitter. In the present study the quenching-rate coefficient is obtained with a single measurement by the use of the dual-beam ASOPS configuration. The theoretical development for dual-beam ASOPS is introduced in the companion paper.[4]

Because of the extremely low UV power produced by our lasers, minor flame species have not been detected. Lasers with suitable UV power are now becoming available, thus making detection of flame radicals possible. We describe the possible use of such lasers.

2. Overview

We discuss the reasons for choosing the ASOPS method in Section 3. In Section 4 we describe the ASOPS instrument that we evaluated in this investigation. The calibrations used to make the ASOPS results quantitative are also described in Section 4. In Section 5 we present the results obtained with the ASOPS instrument. In Section 6 we discuss the importance of these results, and based on these results, we suggest future measurements based on modern mode-locked laser technology.

3. Choice of a Pump–Probe Instrument

Three designs for the pump–probe instrument were examined. The first was based on a single mode-locked laser system. Because of power and modulation considerations, a second design, based on two mode-locked laser systems, was examined. We then modified the dual-laser system by choosing a different timing scheme, which reduced difficulties with pulse-train timing. This final configuration was chosen for the experiments that we describe below.

Consider two pulse trains that overlap in space and time, both tuned in resonance with a population of atoms or molecules. A common implementation of this scenario is the conventional pump–probe instrument.[5,6] Here the pump and the probe beams are derived from the same actively mode-locked laser, and thus both have the same repetition frequency. The pulses are temporally overlapped where they cross in the flame by the use of an optical delay line. The pump is amplitude modulated at frequencies greater than 1 MHz, and the resulting probe modulation is synchronously detected with a high-frequency lock-in amplifier. The amplifier output can be Fourier transformed to obtain power spectral densities. More important, for the excitation scheme shown in Fig. 1(a), the expression for the modulation of the probe beam takes the form[4]

$$\alpha_{\mathrm{MOD}} = \left(\frac{g_3}{g_1}\right)\left[\ln\left(\frac{1}{\sqrt{2}-1}\right)\right]^2 \frac{c^4 A_{21} A_{32} P_{\mathrm{AVE}}{}^{\mathrm{PUMP}} N_T L}{16\pi^3 D^2 h \nu_{12}{}^3 \nu_{23}{}^2 f^L (\Delta\nu_{1/2}{}^L)^2}, \tag{1}$$

where g_i is the degeneracy of the ith electronic state, c is the speed of light (m/s), A_{ji} is the Einstein coefficient for spontaneous emission from level j to level i [in inverse seconds (s^{-1})], $P_{\mathrm{AVE}}{}^{\mathrm{PUMP}}$ is the average laser power of the pump beam [in watts (W)], N_T is the total population density of the resonant atoms [in inverse cubic centimeters (cm^{-3})], L is the interaction length [in centimeters (cm)], D is the focal diameter of both beams in the interaction region (cm), h is Planck's constant [in Joules times seconds (J s)], ν_{ij} is the frequency between the ith and jth levels, f^L is the repetition rate of the lasers (s^{-1}), and $\Delta\nu_{1/2}{}^L$ is the spectral bandwidth of the laser (s^{-1}). Equation (1) demonstrates that for this pump–probe method, collisional effects are absent, in contrast to the laser-induced fluorescence method. However, for diatomic species such as hydroxyl, it is necessary to frequency double the output from the synchronously mode-locked dye laser. Because the modulator can-

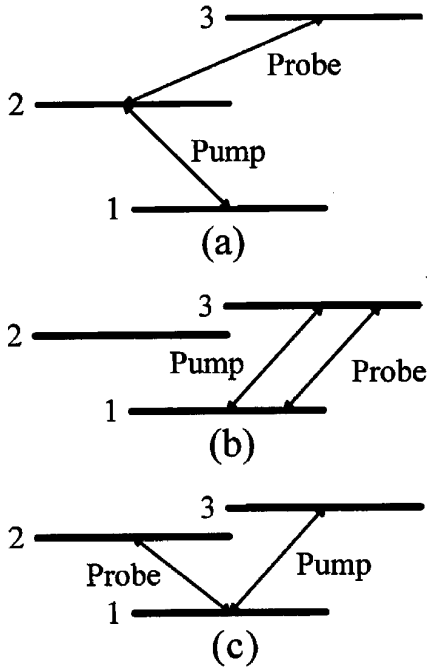

Fig. 1. Example excitation schemes used in pump–probe measurements: (a) pump beam connects electronic levels 1 and 2, and the probe beam connects electronic levels 2 and 3; (b) and (c) examples specific to atomic sodium, where the 1–2 transition represents the D_1 ($3S_{1/2}$–$3P_{1/2}$) line and the 1–3 transition represents the D_2 ($3S_{1/2}$–$3P_{3/2}$) line. In (b), both beams are in resonance with the D_2 line, and in (c), the probe beam is switched to resonance with the D_1 line.

not be used with an UV beam, the dye-laser output must be split into two portions and then frequency doubled. The resulting average power will be in the tens of microwatts,[7] much too small for detection of minor species such as hydroxyl.[4]

To obviate this problem, we evaluated the pump–probe instrument of Fig. 2. Here two actively mode-locked Nd:YAG lasers are frequency doubled, and the output is used to pump two dye lasers synchronously. The mode lockers of both lasers are driven with the same frequency synthesizer (PTS Model 160), so that the ~82-MHz repetition rates of the two laser systems are identical. This requires that adjustments be made to match the cavity lengths of the Nd:YAG lasers. To provide a convenient means of temporally overlapping the pulses from each laser in the interaction volume, a voltage-controlled phase shifter (Merrimac PEW-3-60) is placed between the frequency synthesizer and the mode locker of the pump laser. A variable dc voltage source is used to adjust the phase between the two laser systems. Additional phase adjustments can be made with an optical delay line that the pump-laser beam traverses. The pump beam also passes through a 4-kHz chopper, because this device is easier to operate than an electro-optic modulator. When a low-frequency lock-in amplifier is used to demodulate the probe signal, an impressive SNR results, even though the 4-kHz modulation frequency is located on top of sizable baseband laser noise.[8] Unfortunately, long-term drift of the phases of each laser-pulse train requires constant adjustments in the optical delay line. The chief advantage of this scheme is that at least 1 mW of average UV power is available for both the pump and the probe beams.

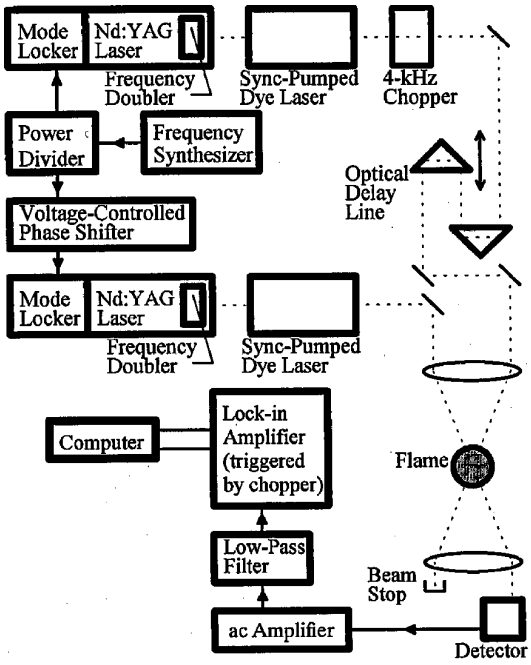

Fig. 2. Conventional pump–probe instrument with two actively mode-locked laser systems. Sync, synchronously.

To retain the 1-mW average UV power, and to eliminate the problem of temporally overlapping two pulse trains emanating from two actively mode-locked lasers, we chose to conduct our experiments with the ASOPS instrument. In this case each laser is actively mode-locked with a separate frequency synthesizer. The synthesizers are operated in a phase-locked, master–slave configuration in which the pump-laser oscillator is also used as the reference oscillator for the probe laser. The lasers are then operated at different repetition frequencies, f^{PUMP} and f^{PROBE}. Thus, as the pump and the probe beams pass through the sample, a beat frequency of $f^{\mathrm{BEAT}} = f^{\mathrm{PUMP}} - f^{\mathrm{PROBE}}$ is impressed onto the probe laser, eliminating the need for amplitude modulation of the pump laser. More important, a controlled repetitive phase walkout of the pump- and the probe-pulse trains occurs in the interaction volume.

The automatic ASOPS phase walkout eliminates the need for an optical delay line or for an electronic phase shifter. Each successive probe pulse is delayed in time (relative to the pump-pulse train) by a constantly increasing duration that is determined by the beat frequency of the system. Thus each probe pulse samples the excited-state population at a slightly later time than the preceding probe pulse. The net effect of the ASOPS technique is that a small amplitude waveform, which is directly related to the fluorescence decay of the species under study, is impressed onto the probe-laser intensity. In essence a temporal transformation of the excited-state decay is performed, with the time scaled by the factor $f^{\mathrm{PUMP}}/f^{\mathrm{BEAT}}$. The process automatically repeats at the period of the ASOPS instrument, which is given by $1/f^{\mathrm{BEAT}}$. The ASOPS technique is thus the optical analog of a sampling oscilloscope. Consequently the ASOPS instrument may potentially permit a large number of averages to be obtained in a time less than that of most turbulent fluctuations (~1 ms).

4. Configuration of the ASOPS Instrument

Having selected the ASOPS method for our instrument, we now describe the details of the instrument and the reasons for choosing the final design. Important considerations include selection of the data-collection rate, changes to the dye lasers since our previous experiments,[3] choice of laser power, and optimization of the detection electronics. The pumping and probing arrangements are also an important consideration, which led us to demonstrate a method that we call dual-beam ASOPS.

A. Data-Collection Rate

The data-collection rate is chosen to maximize the number of averages that can be obtained on the time scale of turbulence, while at the same time the collection frequency is located away from the frequencies of important noise sources. We have previously observed that the beat frequency should be located as far beyond the Nd:YAG power-supply noise as practical.[8] For this reason the ASOPS beat frequency is set at its maximum possible value. We achieved this

Table 1. ASOPS Operating Parameters

Repetition rate	
(f^{PUMP})	81.640000 MHz
(f^{PROBE})	81.484300 MHz
Beat frequency $(f^{BEAT} = f^{PUMP} - f^{PROBE})$	155.700 kHz
Free temporal range $(1/f^{PUMP})$	12.248898 ns
Collection time $(1/f^{BEAT})$	6.42261 μs
Samples per decay (f^{PROBE}/f^{BEAT})	523.34

by maximizing the mode-locking frequency of laser A and minimizing the mode-locking frequency of laser B. The resulting beat frequency of ~160 kHz is limited by the maximum frequency of the natural acoustic resonance of the mode-locking prism for laser A and by the maximum physical cavity length to which the end mirror of laser B can be extended. The resulting ASOPS parameters are summarized in Table 1. A second benefit results from the large beat frequency: the collection time for a single decay is reduced to only 6.42 μs, thus permitting approximately 100 averages within the time scale of turbulence.

B. Laser Considerations

A diagram of the ASOPS instrument is shown in Fig. 3. We again use the laser systems of our previous ASOPS studies,[3] with some slight modifications. Since completion of qualitative ASOPS studies, the stainless-steel dye jets have failed because of excess wear. These jets have been replaced with sapphire jets, resulting in significantly reduced high-frequency noise.[9] A two-plate Lyot filter and an ultrafine étalon (finesse = 2.2) are used for wavelength selection and bandwidth restriction. The laser cavities of both dye lasers are positioned to produce ~20-ps pulses.[8] The resulting bandwidth is at least 1.6×10^{10} Hz[8,10] but is small enough that the *D* lines of sodium are easily resolved. The present trigger system is identical to that of our previous investigation.[3]

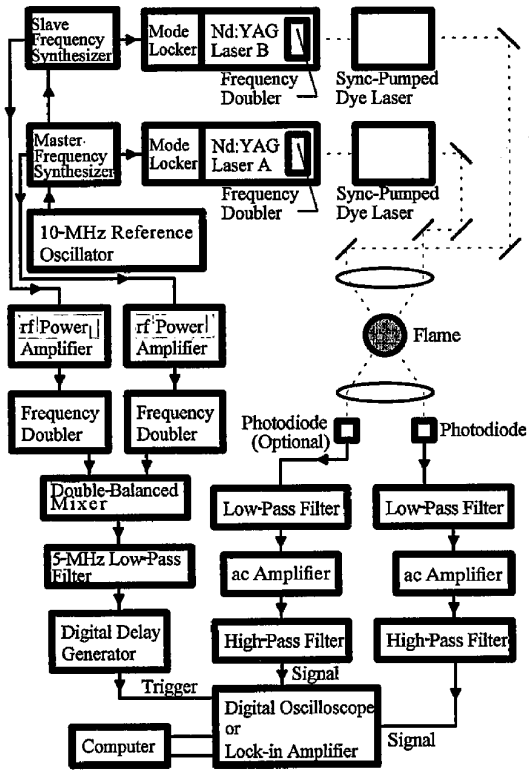

Fig. 3. ASOPS instrument diagram, including the dual-beam option.

To fix the desired power of laser B before the flame, we passed the beam through a Newport 935-5 attenuator, followed by a neutral-density filter. We select the power of laser A by passing the beam through a polarization rotator–polarization beam-splitter combination, followed by a neutral-density filter. The beams are focused in the flame with a 200-mm focal-length lens. For the 2.9° inclusive angle of the present study, the interaction length is 0.15 cm.[4] The resulting beam waist is used along with the present laser-pulse width and bandwidth to estimate a saturation parameter of 850 μW.[4] The saturation parameter is used as a prediction of the onset of saturation.[4] For this reason the pump and the probe power are both set to 700 μW (8.5 pJ/pulse) in the flame. This value is well within the linear range of the photodetector[11] so that no further attenuation of laser B is necessary after the flame. To correct for long-term drift of laser power, both lasers are monitored continuously during ASOPS experiments.

C. Optimization of the Detection Electronics

The photodiode output in Fig. 3 is low-pass filtered by one of three different filters to remove the 82-MHz modulation from the laser. For collection of temporal signals on an oscilloscope, we use either a 20-MHz filter (Trilithic 4LM20-3-CD) or a 50-MHz filter (Texscan 4LE20-CD). When the temporal signal must be taken in the shortest possible time, it becomes necessary to remove as much noise as possible from the ASOPS signal, although a slight amount of distortion is permitted; for these measurements the 20-MHz filter is chosen. Because the 20-MHz filter causes some phase distortion of the signal, the 50-MHz filter is chosen when phase distortion is to be minimized at the expense of total collection time; noise between 20 and 50 MHz must then be reduced by additional signal averaging.[8] For measurements of the magnitude of the fundamental ASOPS beat frequency with a lock-in amplifier, a Texscan 4LM5-3-CD 4-pole low-pass Chebyshev filter with a 5-MHz cutoff frequency is used; in this case phase distortion no longer affects the signal.

The low-pass-filtered photodiode signal is then ac amplified by 1000× with a C-Cor 4375-A ac amplifier. Our lasers produce considerable baseband noise that makes high-pass filtering necessary; in particular, severe switching-power-supply noise is observed near 30 and 60 kHz.[8] For temporal ASOPS studies, the signal is high-pass filtered with a 5-pole 1-kHz Butterworth filter.[12] Attempts to use higher-frequency filters or more poles per filter result in unacceptable

distortion of the temporal signal. Signal averaging is only partially effective in reducing power-supply noise. The averaged noise at the particularly severe frequency of 60 kHz appears as a sine wave on which the ASOPS signal is superimposed. Hence this coherent noise must be reduced further by subtracting it from the temporal ASOPS signal.[8]

For temporal measurements, the high-pass-filtered signal is then fed to a Tektronix 602A digitizing signal analyzer. The *n*-pole digital Bessel filter option of the digitizing signal analyzer is selected to attenuate the remaining high-frequency noise. For lock-in amplifier demodulation of the fundamental ASOPS beat frequency, the ac amplifier output is high-pass filtered with a 7-pole 100-kHz Butterworth filter, which substantially reduces the degradation of the SNR that is caused by the power-supply noise.[12] The filtered signal is then synchronously detected with an EG&G Princeton Applied Research 5202 high-frequency lock-in amplifier, operated with a time constant of 1 s. These dc measurements are used in calibrating the ASOPS instrument.

D. Calibration of the Flame Environment

The chief objective of this study is to demonstrate quantitative concentration measurements with the ASOPS instrument. To this end a second measurement technique, AAS, has been used to calibrate a flame. The AAS method permits absolute concentration measurements, which can then be used to calibrate the ASOPS instrument. In addition the AAS method can be used to verify the linear range of concentrations for ASOPS detection. Finally, the AAS method enables us to measure the collision-broadened sodium linewidth, thus verifying spectral assumptions made in the model in our companion paper.[4]

For the AAS measurements, lamp emission from a tungsten filament lamp is focused through an aperture and then chopped at 4 kHz. The light is then collimated with a second lens and directed to the same set of 200-mm lenses that are used in the ASOPS studies. The light is focused through the center of the flame, 3.3 mm above the burner surface. The light is then collimated and passed through an aperture of less than 5 mm in diameter. The remaining light is then focused into a 0.25-m monochromator. Light from the tungsten lamp is detected with an RCA 1P28 photomultiplier, the output of which is synchronously demodulated with a low-frequency lock-in amplifier.

The premixed methane–air flame is supported by a 1-cm diameter bundle of stainless-steel capillary tubes. The bundle rests on a plastic Perkin–Elmer nebulization chamber, to which a stainless-steel pneumatic nebulizer is attached. The maximum concentration of sodium chloride that was atomized is 10000 μg/ml, because larger concentrations tended to clog the atomizer. The lowest concentration used in AAS measurements is 25 μg/ml, as limited by the discernible change in spectral irradiance. The lowest concentration used for ASOPS detection is 1 μg/ml, because measurements at lower concentrations are hampered by residual Na levels present in the nebulizer chamber. Unfortunately this residual buildup of sodium chloride tends to drift with time. To account for the resulting bias, deionized water is periodically fed to the nebulizer, and the resulting signal is recorded. This signal is then subtracted from the data in software. The magnitude of the residual background signal is an average of 26% of the uncorrected ASOPS signal magnitude for the 1 μg/ml solution.

The flow rates of methane and air are 3.71 and 37.9 ml/s, respectively. Flame stability is increased by the addition of 1.54 ml/s of O_2, resulting in an equivalence ratio of 0.78. To reduce flame fluctuations caused by room air currents, a Hastelloy X slab is placed 21 mm above the burner surface. The equivalent path length[13,14] for this burner is found to be 9.7 mm.

The resulting curve of integrated absorption versus sample concentration was fitted with a linear least-squares procedure for sample concentrations below 177 μg/ml. From the slope of the line, the atomization efficiency was found to be $\varepsilon_{ATOM} = 1.7 \times 10^9 \pm 2 \times 10^6$ cm^{-2} (μg/ml)$^{-1}$. The standard deviation (1σ) in the integrated absorption that results from the fit is 3×10^8 s^{-1}, or approximately 4% of the maximum signal. When the atomization efficiency is divided by the effective path length, a calibration factor of 1.8×10^9 cm^{-3} (μg/ml)$^{-1}$ results. This calibration is used to convert the ASOPS measurements to a quantitative basis.

The integrated absorption versus sample concentration curve for the largest concentrations (>750 μg/ml) was fitted with a nonlinear least-squares technique to determine the collisional width, $(\Delta\nu_{1/2})_c$.[15] The atomization efficiency was taken to be that obtained from the curve fit for optically thin conditions. The resulting collisional linewidth is 2.7×10^9 s^{-1} $\pm$ 3×10^8 s^{-1}, in good agreement with the linewidth measured by Goldsmith.[16] This value is much smaller than the spectral width of the laser (1.6×10^{10} s^{-1}). The fit results in a standard deviation (1σ) in the integrated absorption of 1.5×10^9 s^{-1}, which represents approximately 2% of the maximum signal. Note that the reported error for the collisional linewidth is actually too small, because it does not account for the uncertainty in atomization efficiency.

E. Dual-Beam ASOPS Method

The dependence of the ASOPS signal on collisional effects must be minimized to obtain quantitative results. For rapid data collection, it is necessary to correct for collisional effects in a single measurement. This has resulted in a new excitation scheme for the ASOPS instrument, which we describe below.

If the pump and the probe beams are tuned for the configuration shown in Fig. 1(a), the ASOPS signal

(in volts) is given by[4]

$$S(t) = \eta_d \left(\frac{g_3}{g_1}\right)\left[\ln\left(\frac{1}{\sqrt{2}-1}\right)\right]^2 \frac{c^2 A_{21} A_{32} {P_{\mathrm{AVE}}}^{\mathrm{PUMP}} {P_{\mathrm{AVE}}}^{\mathrm{PROBE}} N_T L \exp[-(Q+A)t]}{4\pi^4 D^4 h {\nu_{12}}^3 {\nu_{23}}^2 f^{\mathrm{PUMP}} f^{\mathrm{PROBE}} \Delta {t_{1/2}}^L (\Delta {\nu_{1/2}}^L)^2}, \tag{2}$$

where η_d is the efficiency of the detection system (in volts per cubic centimeter per watt) Q is the electronic quenching-rate coefficient (s^{-1}); ${P_{\mathrm{AVE}}}^{\mathrm{PUMP}}$ and ${P_{\mathrm{AVE}}}^{\mathrm{PROBE}}$ are the average powers of the pump and the probe lasers (W), respectively, and $\Delta {t_{1/2}}^L$ the temporal pulse width, which is assumed to be identical for both laser beams. Unfortunately most atoms and molecules have additional levels. In particular the $3P$ electronic state of atomic sodium consists of the $3P_{1/2}$ and $3P_{3/2}$ doublet. For this reason one possible excitation scheme is given in Fig. 2(b), in which both beams are tuned to the same line. The resulting ASOPS signal takes the form[4]

$$S(t) = \frac{2}{3}\eta_d \frac{g_3}{g_1}\left(1 + \frac{g_3}{g_1}\right) \frac{c^4 {A_{31}}^2 {P_{\mathrm{AVE}}}^{\mathrm{PUMP}} {P_{\mathrm{AVE}}}^{\mathrm{PROBE}} N_T L\{\exp[-(Q+A)t] + \tfrac{1}{2}\exp[-(Q+A+3Q_{32})t]\}}{\left[\ln\left(\frac{1}{\sqrt{2}-1}\right)\right]^{-2} 4\pi^4 D^4 h {\nu_{13}}^5 f^{\mathrm{PUMP}} f^{\mathrm{PROBE}} \Delta {t_{1/2}}^L (\Delta {\nu_{1/2}}^L)^2}, \tag{3}$$

where Q_{32} is the mixing-rate coefficient between the doublet levels (s^{-1}). Because of the simplicity of tuning both lasers to the same wavelength, this detection scheme is used in some of the experiments described below. However, it is impossible to correct for collisional effects with a single measurement because there are now two unknowns, Q and Q_{32}.

To obviate this difficulty, we have developed the dual-beam ASOPS method. The theory behind this method is given in the companion paper.[4] If the lasers are tuned to the configuration shown in Fig. 2(c), then both the pump and the probe beams will be modulated. Thus the common distinction between pump and probe loses its meaning. Detection of the pump beam will result in a signal given by[4]

$$S(t) = \frac{2}{3}\eta_d \frac{c^4 A_{31} A_{21} {P_{\mathrm{AVE}}}^{\mathrm{PUMP}} {P_{\mathrm{AVE}}}^{\mathrm{PROBE}} N_T L\{2\exp[-(Q+A)t] + \exp[-(Q+A+3Q_{32})t]\}}{\left[\ln\left(\frac{1}{\sqrt{2}-1}\right)\right]^{-2} 4\pi^4 D^4 h {\nu_{12}}^3 {\nu_{13}}^2 f^{\mathrm{PUMP}} f^{\mathrm{PROBE}} \Delta {t_{1/2}}^L (\Delta {\nu_{1/2}}^L)^2}, \tag{4}$$

whereas detection of the probe beam results in a signal given by[4]

$$S(t) = \eta_d \frac{c^4 A_{31} A_{21} {P_{\mathrm{AVE}}}^{\mathrm{PUMP}} {P_{\mathrm{AVE}}}^{\mathrm{PROBE}} N_T L \exp[-(Q+A)t]}{\left[\ln\left(\frac{1}{\sqrt{2}-1}\right)\right]^{-2} 4\pi^4 D^4 h {\nu_{12}}^2 {\nu_{13}}^3 f^{\mathrm{PUMP}} f^{\mathrm{PROBE}} \Delta {t_{1/2}}^L (\Delta {\nu_{1/2}}^L)^2}. \tag{5}$$

Thus simultaneous detection of both beams yields both unknown quantities, Q and Q_{32}, within the time scale of turbulence. Moreover, because the degeneracies of the ground and the electronic states connected by the probe beam are equal, the resulting signal on the probe depends on only Q (and Q_{32} is absent).[4]

For the dual-beam ASOPS measurements, both laser A and laser B can be detected with individual EG&G FND-100Q photodiodes (see Fig. 3). The photodiode outputs can then be filtered and amplified. This measurement would be necessary if both Q and Q_{32} were desired in a turbulent flame environment. However, only Q is needed in the present study. This is fortunate, because laser A happens to produce significantly more noise than laser B,[8] and only a single wideband ac amplifier is available in our laboratory. In the present experiment Q can be obtained by tuning laser A to the D_2 line of sodium and detecting laser B, which is tuned to the D_1 line. Thus the second detection system shown in Fig. 3 is optional, and only the signal from laser B is measured in the present studies. In future studies the simultaneous detection scheme would add little complexity to the ASOPS instrument.

5. Experimental ASOPS Results

The present ASOPS experiments can be divided into three categories. In all studies data are taken while the sodium concentration is varied in a flat flame burner. In the first category of experiments, the

optically thin range is determined for the ASOPS instrument by the use of the dc measurement system with a lock-in amplifier. The results are used to demonstrate the quantitative nature of the ASOPS method. We then pursue two categories of temporal measurements. In the second category of experiments, data-collection time is of primary concern. Only 128 averages are taken for each concentration, corresponding to a collection time that falls within the turbulent temporal scale of ~1 ms or less. For simplicity both laser A and laser B are set to the D_2 transition at 589.00 nm, as verified with a Burleigh Wavemeter Jr. Laser B is then detected because its noise is more favorable than that of laser A. Finally, in the third category of experiments, we demonstrate the dual-beam ASOPS method.

A. Quantitative ASOPS Results

The ASOPS results obtained with a lock-in amplifier are shown in Figs. 4 and 5. The average ASOPS values result in significantly less scatter from linearity than the AAS calibration. This is demonstrated by the superimposed linear least-squares fit, which results in a standard deviation of only 1.0% of the maximum signal. This deviation is represented by the 68% confidence interval of Fig. 4. The actual fluctuation in the experimental data is much larger, as shown by the confidence intervals in Fig. 5. These intervals represent the sample standard deviations at each point; each point is the average of 3 to 5 individual samples. Nearly all the observed deviation is caused by long-term drift in the wavelength of the lasers.

The effects of extreme optical thickness on the ASOPS signal are also demonstrated in Fig. 5. In Fig. 5 the ASOPS signal begins to fall with increasing concentration, unlike the AAS signal, which continues to increase. This can pose an unforeseen difficulty in interpreting ASOPS data: it is possible for a given ASOPS signal level to correspond to two different concentrations. For this reason it is recommended that the transmission of the pump laser be detected after the flame, because the present instrument is not appropriate for optically thick flames. This was not done in the present study because of the well-characterized flame environment.

Both AAS and ASOPS are similar on a theoretical basis because the incident light in each case has a spectral width that is large compared with the linewidth of the individual sodium *D* lines. Thus the optically thin regime for ASOPS should also end at or below approximately 177 μg/ml. However, the effective ASOPS interaction length is only 0.15 cm for the present geometry. Because the center of the interaction volume is placed approximately 3 mm beyond the burner center, both the pump and the probe beams must traverse much of the flame before they cross. Consequently, when optically thick conditions are present, the pump and the probe irradiance at the crossing volume will be greatly attenuated from the irradiance values that are incident upon the leading edge of the flame. The resulting ASOPS signal should also be reduced, unlike the AAS signal, which continues to increase as the sodium concentration surpasses 177 μg/ml. Hence the ASOPS method should serve as a much better indicator of the onset of nonlinear conditions. This might not be true if the crossing volume had been positioned near the front edge of the flame. In Fig. 4 the linear regime for ASOPS is shown to end between a concentration of 100 and 177 μg/ml. This is indeed a somewhat lower concentration than that found for the AAS study.

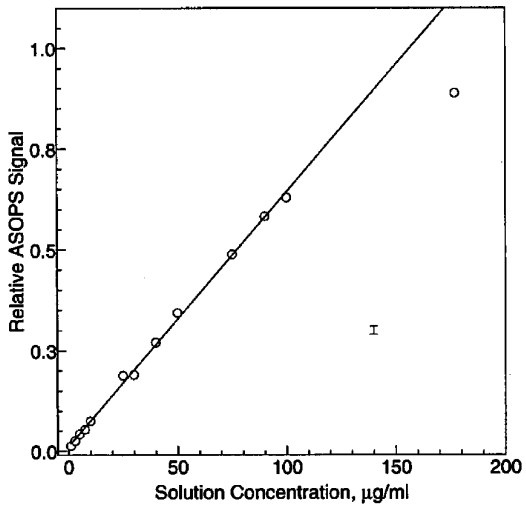

Fig. 4. Variation of the ASOPS signal with atomized solution concentration. The line is a linear least-squares fit to those points that have a concentration less than or equal to 100 μg/ml. The point at 177 μg/ml is plotted to emphasize the departure from linearity. The confidence interval (I) represents the standard deviation (1σ) of the data from the line. The actual deviation for each point is much larger, as shown in Fig. 5, below.

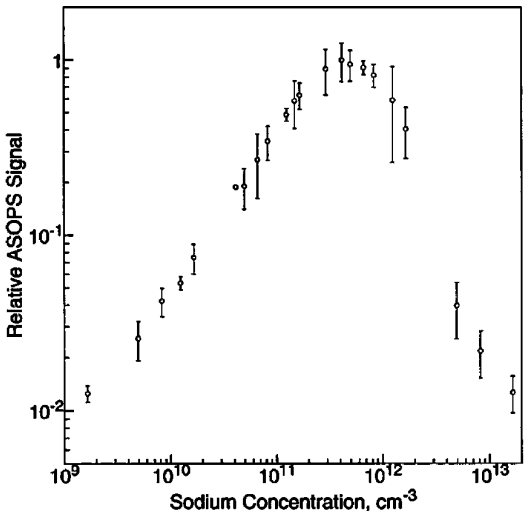

Fig. 5. Variation of the ASOPS signal with sodium number density, calculated from the AAS calibration parameter. Each point is an average of several points, ranging from three to five values. For this reason the confidence intervals represent the sample standard deviation (1σ).

B. Rapid Collection of Temporal ASOPS Data

Having determined the extent of the linear range, we shifted the experimental emphasis to temporal studies. An ASOPS signal obtained with only 128 averages for a 100 μg/ml solution is shown in Fig. 6. The Tektronix 602A digital oscilloscope is operated in the real-time acquisition mode. The resulting peak SNR is approximately 10:1. For similar temporal signals, the 1:1 SNR point is found to occur at ~3 μg/ml. This detection limit is largely a result of 2-MHz rf interference.[8] The maximum photodiode output signal at 3 μg/ml is only ~5 μV. When we multiply the solution concentration by the AAS calibration factor, the sodium number density is found to be 5.3×10^9 cm^{-3}. The effects of additional signal averaging at low sodium concentrations are minimal. With 1024 averages for this concentration, the quantizer resolution limits the peak SNR to ~4:1. The experimental value of the detection limit is ~5 orders of magnitude larger than that corresponding to the shot-noise limit with a 1-Hz collection rate.[4] Taking into account the different collection times, we show that the performance of the present instrument is slightly less than 4 orders of magnitude worse than that corresponding to the shot-noise limit.

C. Dual-Beam ASOPS Results

To simplify the measurement of Q, we use the dual-beam ASOPS excitation method. The 50-MHz low-pass filter is chosen to minimize distortion, and 8192 averages are taken. This amount of averaging is not necessary to obtain a decay but is sufficient to ensure a reliable estimate of Q. Coherent noise from the Nd:YAG laser power supplies is measured and subtracted from the signals before the curve fit is performed for Q.[8] We again use a 100-μg/ml NaCl solution. Two points are taken: one at the burner center and one 4 mm from the burner center. The resulting $3P$ lifetimes obtained with Eq. (5) are 950 and 780 ps, respectively, for the two points. This range is in excellent agreement with the value of 830 ps measured by Fourkas *et al.*[17] with a picosecond transient-induced-grating method.[18] The variation of measured values of Q with radial position along the burner for the present flat flame is found to be 18%.

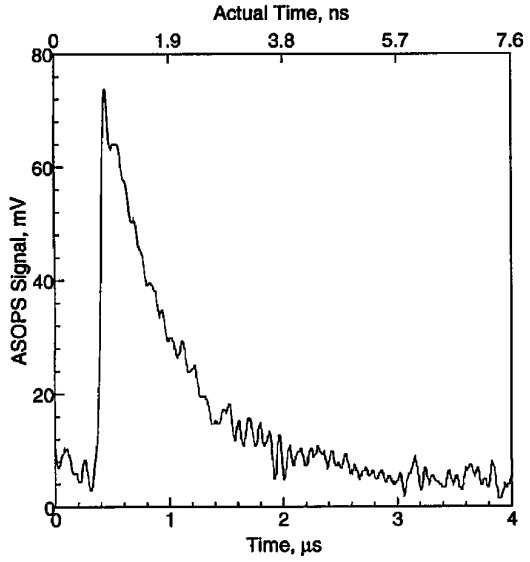

Fig. 6. ASOPS decay obtained with 128 averages. A 100-μg/ml solution was atomized inito the flame.

6. Discussion

In a companion paper,[4] we estimate a detection limit for both sodium and hydroxyl by assuming a 10^{-8} depth of modulation. The present minimum modulation depth is clearly not this small. However, the ratio between the hydroxyl and sodium estimates will remain unchanged, no matter what the assumed value of the modulation depth may happen to be.[4] By multiplying the present sodium detection limit by this ratio (3.8×10^7), we estimate a detection limit of 2×10^{17} cm^{-3} for the hydroxyl radical. This calculation is based on the assumption that the $Q_1(9)$ line of $A\,^2\Sigma^+$ $(v' = 0)$–$X\,^2\Pi^+$ $(v'' = 0)$ hydroxyl is detected in a flame at 2000 K and that 1 mW of average pump and probe power is used for both hydroxyl and sodium. For sodium this laser power is chosen to preclude saturation.[4] In the case of hydroxyl, the saturation parameter increases to 900 mW.[4] The 1-mW value is chosen in the present calculation because it is a conservative estimate of the available UV laser power.[7] Any future improvements in laser technology that result in a substantial increase in UV laser power will clearly improve the detection limit for hydroxyl. In addition, our present detection limit is determined primarily by noise in the detection electronics. Therefore an increase in signal that accompanies a greater laser power would directly increase the SNR until shot noise from the probe laser becomes important. The expression for the ASOPS signal in Eq. (2) indicates that the SNR will thus increase in direct proportion to the pump and the probe power, provided the bandwidth and pulse width remain unchanged.

The lasers used in our experiments have many undesirable characteristics compared with the technology that is now commercially available, and new mode-locked laser systems based on Ti:sapphire technology may eliminate these characteristics. Kafka *et al.*[19] found that a mode-locked Ti:sapphire laser can produce pulse widths that are selectable from 40 fs to 100 ps, with an average output power over 3.5 W for the entire range of pulse widths at a wavelength of 780 nm. Nebel and Beigang[20] obtained output powers of 700, 120, and 10 mW at wavelengths of 410, 272, and 210 nm by the use of second-, third-, and fourth-harmonic generation, respectively. The pulse width that they used was 1.4 ps. They were able to obtain radiation over a continuous range extending from 205 to 525 nm. This range covers the electronic resonances of many important flame radicals.

The laser power from Ti:sapphire lasers is thus over 2 orders of magnitude larger than the lasers that we use in our present experiments and up to a factor

of 700 greater for CH, which absorbs at ~430 nm. Consequently the detection limit for radical species could be improved by up to 4 orders of magnitude when Ti:sapphire lasers are used, yielding a bounding value of 2×10^{13} cm^{-3}. However, our present pulse width is 20 ps, which compares with the 1.4-ps pulse width used in the Ti:sapphire demonstrations of Nebel and Beigang,[20] although pulse widths of over 20 ps are possible.[19] If the same power levels are not possible with 20-ps pulses, the above estimate of the detection limit would have to be adjusted accordingly.

We are not aware of any noise comparisons between mode-locked Ti:sapphire lasers and mode-locked Nd:YAG lasers. However, the noise from a mode-locked Ti:sapphire laser has been found to be favorable when compared with the noise from a colliding-pulse mode-locked dye laser.[21]

Rapid lifetime measurements are also possible by the use of the new laser technology in conjunction with the ASOPS method. Kafka *et al.*[22] operated two mode-locked Ti:sapphire lasers in the ASOPS configuration, obtaining an impressive cross correlation of 150 fs. This compares with a value of 7 ps for our lasers.[23] Based on the detection limits of our present results, along with the improved laser performance reported by Kafka *et al.*[22] and by Nebel and Beigang,[20] we believe that picosecond pump–probe spectroscopy remains promising as a practical concentration diagnostic for flame radicals in turbulent flames.

Despite the success of our present experiments, the pump–probe absorption method may not be the best choice in many applications. On the other hand, the ASOPS timing scheme can be used to observe any interaction process between light and molecules. Linne and Fiechtner[24] have recently demonstrated degenerate four-wave mixing (DFWM) measurements in a flame with a single 82-MHz regeneratively mode-locked Ti:sapphire laser. The ASOPS technique would make it possible to obtain additional information rapidly with DFWM, including ground-state collision rates, diffusion constants, velocities, and excited-state dephasing rates.[17] Moreover, the potential for zero-background signals could vastly improve the SNR when the ASOPS scheme is used with DFWM. Time-resolved fluorescence with picosecond excitation has recently been demonstrated for atomic sodium in an atmospheric flame and remains a promising technique for minor flame species.[25]

7. Summary

We have successfully demonstrated the first quantitative evaluation of the ASOPS technique in a flame environment. ASOPS data are taken on a time scale that is adequate for many turbulence applications and at the same time yields an impressive SNR under optically thin conditions. Based on a measured detection limit for atomic sodium, we estimate that the detection limit for the $Q_1(9)$ line of $A\,^2\Sigma^+(v' = 0)$–$X\,^2\Pi^+$ $(v'' = 0)$ hydroxyl is 2×10^{17} cm^{-3}. Although this concentration is approximately 1 to 2 orders of magnitude too large for practical flame studies, new mode-locked Ti:sapphire lasers may provide the power necessary to obtain a lower detection limit.

The dual-beam ASOPS excitation method has been demonstrated for the first time. We find that the quenching-rate coefficient for atomic sodium can be obtained in a single measurement with this configuration. The measured values of Q are in excellent agreement with those reported in the literature. In addition the ASOPS timing scheme is not limited to absorption and stimulated emission and may prove to be useful with other techniques such as DFWM.

The authors thank Fred Lytle, Department of Chemistry, Purdue University, for the loan of much of the equipment for the present study. This work was sponsored by the Office of Scientific Research, U.S. Air Force Systems Command, under grant AFOSR-89-0051.

References

1. R. S. Barlow, R. W. Dibble, and R. P. Lucht, "Simultaneous measurement of Raman scattering and laser-induced OH fluorescence in nonpremixed turbulent jet flames," Opt. Lett. **14,** 263–265 (1989).
2. N. H. Wrobel and N. H. Pratt, "Laser-induced sodium fluorescence measurements in a turbulent propane diffusion flame," in *Seventeenth Symposium (International) on Combustion* (*Combustion Institute, Pittsburgh, Pa., 1978*), *pp. 957–966.*
3. G. J. Fiechtner, G. B. King, N. M. Laurendeau, and F. E. Lytle, "Measurements of atomic sodium in flames by asynchronous optical sampling: theory and experiment," Appl. Opt. **31,** 2849–2864 (1992).
4. G. J. Fiechtner, G. B. King, and N. M. Laurendeau, "A rate equation model for quantitative concentration measurements in flames by picosecond pump–probe absorption spectroscopy," Appl. Opt. **33,** 1108–1116 (1994).
5. A. J. Langley, R. A. Beaman, J. Baran, A. N. Davies, and W. J. Jones, "Concentration-modulated absorption spectroscopy," Opt. Lett. **10,** 327–329 (1985); A. J. Langley, R. A. Beaman, A. N. Davies, W. J. Jones, and J. Baran, "Concentration-modulated absorption spectroscopy I," Chem. Phys. **101,** 117–125 (1986); R. A. Beaman, A. N. Davies, A. J. Langley, W. J. Jones, and J. Baran, "Concentration-modulated absorption spectroscopy: II. Temporal variation of gain," Chem. Phys. **101,** 127–132 (1986).
6. B. A. Mann, "Novel coherent laser spectroscopic techniques for minor species combustion diagnostics," Ph.D. dissertation (University of Reading, Whiteknights, Reading, Berks., England, 1991).
7. G. J. Fiechtner, G. B. King, N. M. Laurendeau, R. J. Kneisler, and F. E. Lytle, "Efficient frequency doubling for synchronously mode-locked dye lasers," Appl. Spectrosc. **43,** 1286–1287 (1989).
8. G. J. Fiechtner, "Quantitative concentration measurements in atmospheric-pressure flames by picosecond pump/probe absorption spectroscopy," Ph.D. dissertation (Purdue University, West Lafayette, Ind., 1992).
9. H. P. Härri, S. Leutwyler, and E. Schumacher, "Nozzle design yielding interferometrically flat fluid jets for use in single-mode dye lasers," Rev. Sci. Instrum. **53,** 1855 (1982).
10. G. J. Blanchard and M. J. Wirth, "Transform-limited behavior from the synchronously pumped cw dye laser," Opt. Commun. **53,** 394–400 (1985).
11. P. A. Elzinga, "Asynchronous optical sampling," M.S. thesis (Purdue University, West Lafayette, Ind., 1986).

12. A. I. Zverev, *Handbook of Filter Synthesis* (*Wiley, New York, 1967*).
13. C. D. Carter, "Saturated fluorescence measurements of the hydroxyl radical in laminar high-pressure flames," Ph.D. dissertation (Purdue University, West Lafayette, Ind., 1990).
14. R. P. Lucht, D. W. Sweeney, and N. M. Laurendeau, "Laser-saturated fluorescence measurements of OH in atmospheric pressure of $CH_4/O_2/N_2$ flames under sooting and non-sooting conditions," Combust. Sci. Technol. **42,** 259–281 (1985).
15. C. Th. J. Alkemade, Tj. Hollander, W. Snelleman, and P. J. Th. Zeegers, *Metal Vapours in Flames* (Pergamon, New York, 1982).
16 J. E. M. Goldsmith, "Spatially resolved saturated absorption spectroscopy in flames," Opt. Lett. **6,** 525–527 (1981).
17. J. T. Fourkas, T. R. Brewer, H. Kim, and M. D. Fayer, "Picosecond time-resolved four-wave mixing experiments in sodium-seeded flames," Opt. Lett. **16,** 177–179 (1991).
18. R. P. Lucht, R. Trebino, and L. A. Rahn, "Resonant multiwave mixing spectra of gas phase sodium: non-perturbative calculations," Rep. SAND91-8556 (Sandia National Laboratories, Livermore, Calif., 1991).
19. J. D. Kafka, M. L. Watts, and J. W. Pieterse, "Picosecond and femtosecond pulse generation in a regeneratively mode-locked Ti:sapphire laser," IEEE J. Quantum Electron. **28,** 2151–2162 (1992).
20. A. Nebel and R. Beigang, "External frquency conversion of cw mode-locked $Ti:Al_2O_3$ laser radiation," Opt. Lett. **16,** 1729–1731 (1991).
21 J. Son, J. V. Rudd, and F. Whitaker, "Noise characterization of a self-mode-locked Ti:sapphire laser," Opt. Lett. **17,** 733–735 (1992).
22. J. D. Kafka, J. W. Pieterse, and M. L. Watts, "Two-color subpicosecond optical sampling technique," Opt. Lett. **17,** 1286–1288 (1992).
23. P. A. Elzinga, R. J. Kneisler, F. E. Lytle, Y. Jiang, G. B. King, and N. M. Laurendeau, "Pump/probe method for fast analysis of visible spectral signatures utilizing asynchronous optical sampling," Appl. Opt. **26,** 4303–4309 (1987); R. J. Kneisler, F. E. Lytle, G. J. Fiechtner, Y. Jiang, G. B. King, and N. M. Laurendeau, "Asynchronous optical sampling: a new combustion diagnostic for potential use in turbulent, high-pressure flames," Opt. Lett. **14,** 260–262 (1989).
24. M. A. Linne and G. J. Fiechtner, "Picosecond degenerate four-wave mixing of potassium in a methane–air flame," Opt. Lett. **19,** 667–669 (1994).
25. M. S. Klassen, B. D. Thompson, T. A. Reichardt, G. B. King, and N. M. Laurendeau, "Flame concentration measurements using picosecond time-resolved laser-induced fluorescence," Combust. Sci. Technol. **97,** 391–403 (1994).